Video Article

Well-aligned Vertically Oriented ZnO Nanorod Arrays and their Application in Inverted Small Molecule Solar Cells

Ming-Yi Lin[1], Shang-Hsuan Wu[2], Li-Jen Hsiao[3], Widhya Budiawan[2], Shih-Lun Chen[4], Wei-Chen Tu[4], Chia-Yen Lee[1], Yia-Chung Chang[2], Chih-Wei Chu[2]

[1]Department of Electrical Engineering, National United University

[2]Research Center of Applied Science, Academia Sinica

[3]Department of Graduate Institute of Photonics and Optoelectronics, National Taiwan University

[4]Department of Electronic Engineering, Chung Yuan Christian University

Correspondence to: Chih-Wei Chu at gchu@gate.sinica.edu.tw

URL: https://www.jove.com/video/56149
DOI: doi:10.3791/56149

Keywords: Engineering, Issue 134, ZnO nanorod arrays, AZO, ZnO, small molecule, inverted solar cells, sol-gel, sputtered

Date Published: 4/25/2018

Citation: Lin, M.Y., Wu, S.H., Hsiao, L.J., Budiawan, W., Chen, S.L., Tu, W.C., Lee, C.Y., Chang, Y.C., Chu, C.W. Well-aligned Vertically Oriented ZnO Nanorod Arrays and their Application in Inverted Small Molecule Solar Cells. *J. Vis. Exp.* (134), e56149, doi:10.3791/56149 (2018).

Abstract

This manuscript describes how to design and fabricate efficient inverted solar cells, which are based on a two-dimensional conjugated small molecule (SMPV1) and [6,6]-phenyl-C71-butyric acid methyl ester ($PC_{71}BM$), by utilizing ZnO nanorods (NRs) grown on a high quality Al-doped ZnO (AZO) seed layer. The inverted SMPV1:$PC_{71}BM$ solar cells with ZnO NRs that grew on both a sputtered and sol-gel processed AZO seed layer are fabricated. Compared with the AZO thin film prepared by the sol-gel method, the sputtered AZO thin film exhibits better crystallization and lower surface roughness, according to X-ray diffraction (XRD) and atomic force microscope (AFM) measurements. The orientation of the ZnO NRs grown on a sputtered AZO seed layer shows better vertical alignment, which is beneficial for the deposition of the subsequent active layer, forming better surface morphologies. Generally, the surface morphology of the active layer mainly dominates the fill factor (FF) of the devices. Consequently, the well-aligned ZnO NRs can be used to improve the carrier collection of the active layer and to increase the FF of the solar cells. Moreover, as an anti-reflection structure, it can also be utilized to enhance the light harvesting of the absorption layer, with the power conversion efficiency (PCE) of solar cells reaching 6.01%, higher than the sol-gel based solar cells with an efficiency of 4.74%.

Video Link

The video component of this article can be found at https://www.jove.com/video/56149/

Introduction

Organic photovoltaic (OPV) devices have recently undergone remarkable developments in the application of renewable energy sources. Such organic devices have many advantages, including solution-process compatibility, low cost, light weight, flexibility, *etc.*[1,2,3,4,5] Up until now, polymer solar cells (PSCs) with a PCE of more than 10% have been developed by utilizing the conjugated polymers blended with $PC_{71}BM$[6]. Compared to polymer-based PSCs, small molecule-based OPVs (SM-OPVs) have attracted more attention when it comes to fabricating OPVs due to their several distinct advantages, including well-defined chemical structures, facile synthesis and purification, and generally higher open-circuit voltages (V_{oc})[7,8,9]. At present, a 2-D structure conjugated small molecule SMPV1 (2,6-Bis[2,5-bis(3-octylrhodanine)-(3,3-dioctyl-2,2':5,2''-terthiophene)]-4,8-bis((5-ethylhexyl)thiophen-2-yl)benzo[1,2-b:4,5-b']dithiophene) with BDT-T (benzo[1,2-b:4,5-b']dithiophene) as the core unit and 3-octylrodanine as the electron-withdrawing end-group[10] has been designed and used to blend with $PC_{71}BM$ for promising sustainable OPVs application. The PCE of conventional small molecule solar cells (SM-OPVs) based on SMPV1 blended with $PC_{71}BM$ has reached more than 8.0%[10,11].

In the past, PSCs could be enhanced and optimized simply by adjusting the thickness of the active layer. However, unlike PSCs, SM-OPVs in general have a shorter diffusion length, which greatly limits the thickness of the active layer. Hence, to further increase the short current density (J_{sc}) of SM-OPVs, utilizing the nano-structure[12] or NRs[9] to improve optical absorption of SM-OPVs became necessary.

Among these methods, the anti-reflection NRs structure is generally effective for light harvesting of the active layer over a broad range of wavelengths; therefore, knowing how to grow well-aligned vertically oriented zinc oxide (ZnO) NRs is very critical. The surface roughness of the seed layer below the ZnO NRs layer has a great influence on the orientation of the NR arrays; therefore, in order to deposit well-oriented NRs, the crystallization of the seed layer needs to be precisely controlled[9].

In this work, the AZO films are prepared by theRadio-Frequency (RF) sputtering technique. Compared with other techniques, RF sputtering is known to be an efficient technology that is transferable to industry for it is a reliable deposition technique, which allows the synthesis of high purity, uniform, smooth, and self-sustainable AZO thin films to grow over large area substrates. Utilizing the RF sputtering deposition enables the forming of high quality AZO films that exhibit high crystallization with reduced roughness of surface. Therefore, in the subsequent growth layer,

the orientations of the NRs are highly aligned, even more so when compared to ZnO films prepared by the sol-gel method. Using this technique, the PCE of the inverted small molecule solar cells based on well-aligned vertically oriented ZnO NR arrays can reach 6.01%.

Protocol

1. Growth of AZO Sputtered Seed Layer on ITO Substrate

1. Stick 4 anti-corrosion tape pieces (0.3 x 1.5 cm) on one side of the indium tin oxide (ITO) substrate to form a square (1.5 x 1.5 cm). Put the ITO into hydrochloric acid for 15 min to etch the exposed area of ITO.
2. Remove the tape and clean the sample using a sonicator; sonicate with deionized (DI) water, acetone, ethanol, and isopropanol in turn for 30 min each. Blow-dry the patterned ITO with a compressed nitrogen gun.
3. Attach the cleaned patterned ITO substrates onto the substrate holder by tape, and load the holder into the main chamber of RF sputtering system. Pump the chamber pressure to below 4 x 10^{-6} torr via the mechanical and diffusion pump to ensure environmental purity.
4. Insert pure argon gas (flow rate: 30 sccm) into the main chamber and control the pump to maintain the pressure of chamber at 1 mtorr.
5. Prepare the AZO seed layers using the RF (13.56 MHz) sputtering method, based on the reported method[13]. Use a circular 2 in dimension AZO (2 wt% Al_2O_3 in ZnO) ceramic target to deposit them onto pre-cleaned ITO glass substrates. Keep the target-to-substrate distance at 10 cm.
6. Maintain working pressure at 1 mtorr and RF power at 40 W during the deposition. Control the substrate temperature at room temperature. Set the applied DC bias and deposition rate to 187 V and 4 nm/min, respectively to deposit the AZO thin film. The thickness of the AZO seed layer should be controlled at 40 nm based on the quartz crystal thickness monitor.
7. After the sample cools down to 30 °C in the chamber, turn off the pump and insert nitrogen gas into the main chamber until the chamber can be opened. Remove the sample from the substrate holder.

2. Growth of the Sol-gel Processed ZnO Seed Layer on ITO Substrate

1. Deposit the ZnO seed layer on the patterned ITO substrate by the sol-gel spin coating method[14]. The zinc acetate dihydrate, 2-methoxethanol, and monoethanolamine (MEA) are used as the starting materials, solvent, and stabilizer, respectively.
    1. Dissolve the zinc acetate dihydrate (4.39 g) in a mixture of 2-methoxethanol (40 mL) and MEA (1.22 g) to obtain the zinc acetate concentration of 0.5 M.
    2. Stir the resulting mixture at 60 °C for 2 h. Let the sol sit for 12 h to form a clear and transparent homogeneous solution.
    3. Deposit the ZnO seed layer onto cleaned ITO patterned glass substrates using the spin coating method. Add 0.1 mL sol-gel solution onto the substrate and rotate at 3,000 rpm for 30 s using a spin coater.
    4. After spin coating, dry the film at 200 °C for 30 min on a hot plate to allow the solvent to evaporate and remove the organic residues. The thickness of the ZnO seed layer should be around 40 nm[14].

3. Growth of ZnO NR Array on a Seed Layer

1. Grow the ZnO NR array using the hydrothermal method.
    1. Mix 1.49 g zinc nitrate hexahydrate ($Zn(NO_3)_2{\cdot}6H_2O$) and 0.7 g hexamethylenetetramine (HMT) ($C_6H_{12}N_4$) in 100 mL DI water. Stir the resulting mixture at room temperature for 30 min.
    2. Attach the ITO side of the AZO sputtered seed layer with the ZnO sol-gel samples to the cover glass using tape. Put the samples in a 50 mL polypropylene conical tube filled with the 50 mL solution of $Zn(NO_3)_2{\cdot}6H_2O$ and HMT.
    3. During the growth, heat the polypropylene conical tube by laying it horizontally in a laboratory oven with the spin coated samples facing downward, and maintain the temperature at 90 °C for 90 min.
    4. At the end of the growth period, remove the substrates from the solution and immediately rinse the sample surface with DI water and ethanol (inside two wash bottles) in turn for 1 min each to remove residual salt from the surface. Blow-dry the sample using a compressed nitrogen gun and bake it on a hot plate at 250 °C for 10 min.

4. Fabrication and Measurement of Inverted Small Molecule Solar Cells

1. Load the ITO substrate with the ZnO NR array onto a spin coater in the glovebox. Mix 1 mL of toluene containing 15 mg of SMPV1 and 11.25 mg of $PC_{71}BM$. Add 0.1 mL solution, spin the sample at 2,000 rpm for 40 s using a spin coater, and anneal it at 60 °C for 2 min.
2. After the annealing process, place the substrate in a thermal evaporation system. Pump the vacuum chamber initially using a mechanical pump until the pressure reaches 4 x 10^{-2} torr, then switch to a turbo pump to make the ambient pressure < 4 x 10^{-6} torr.
3. Deposit the MoO_3 layer at a deposition rate of 0.1 nm/s by heating MoO_3 powder in a resistive molybdenum boat with a Z-ratio of 1.0 and an input current of 105 A. Deposit the Ag layer at a deposition rate of 0.5 nm/s by heating silver ingot in a resistive tungsten boat with a Z-ratio of 0.529 and an input current of 190 A. The system should include a quartz crystal evaporation rate monitor for controlling the evaporation process. The thickness of the MoO_3 and Ag layers should be controlled to be 5 and 150 nm, respectively based on the quartz crystal thickness monitor.
4. After the sample cools down to 30 °C in the chamber, turn off the pump, and insert nitrogen gas into the chamber until the chamber can be opened. Remove the sample from the substrate holder and load the sample into the glovebox.
5. Open the solar simulator system and wait 20 min until the light source of the system is stable. Illuminate the sample at 100 mW/cm^2 from a solar simulator using an air mass 1.5 global (AM 1.5G) filter. Simultaneously, use the analyzer to sweep the device from -1 V to +1 V to obtain the current density-voltage (J-V) curve[14,15].

5. Characterization Techniques

1. Perform the X-ray diffraction measurment[16] with a Cu Kα source to study the structures of the ZnO NRs, on the AZO sputtered seed layer and the ZnO sol-gel processed seed layer. The scan speed should be 1 °/min, and the scan range should be 10-90 ° (2θ).
2. Characterize the surface morphology and cross-sectional image of the samples by field emission scanning electron microscopy[17] by setting the operating voltage at 10 kV.
3. Obtain the micro photoluminescence (PL) spectra of all of the samples using a 325 nm He-Cd CW laser (20 mW) as the excitation source with a 2,400 grooves/mm grating in the backscattering geometry. AllPL measurements[18] should be performed at room temperature.

Representative Results

The layered structure of the devices consisted of an ITO substrate/AZO (40 nm)/ZnO NRs layer, SMPV1:$PC_{71}BM$ (80 nm)/MoO_3 (5 nm)/Ag (150 nm) as shown in **Figure 1**. In general, the AZO or ZnO seed layer is widely used to function as the electron transport layer (ETL) in PSCs devices. Apart from PSCs, SM-OPVs usually have a shorter active layer, limited by the shorter diffusion length[8]. Hence, to further improve the light-harvesting capability of devices, the ZnO NRs layer is introduced to be grown on the seed layer, to work as an anti-reflection layer to enhance collection of the incident light, and to increase the interface area for carrier collection at the same time[12,14].

The surface morphology and roughness of the seed layer have a significant influence on the orientation of the NR arrays. **Figure 2a** and **Figure 2b** areAFM images of the seed layer based on the sputtering method and the sol-gel method, respectively. The surface morphology of the sol-gel processed seed layer can be seen to not only exhibit higher roughness, but also to form a natural ridge pattern. As a result, the orientation of the NR arrays grown on the sol-gel processed layer will be much rougher than layers grown using the sputtering technique. **Figure 2c** and **Figure 2d** show the scanning electron microscope (SEM) images of the NR arrays grown on the sputtered seed layer and the sol-gel processed seed layer respectively. Clearly, the orientation of the NR arrays grown on the sputtered AZO layer can be observed to be better than those grown on the sol-gel processed ZnO layer.

In addition to the SEM images, to further estimate the orientation of the NR arrays, XRD analysis (**Figure 3**) is used to identify the orientation and crystallization of the NR arrays. Compared with the XRD spectra of the NRs grown on a sol-gel processed seed layer, the spectra of NR arrays based on a sputtered seed layer show a relatively stronger peak at 34.5 °, indicating that not only the orientation but also the crystallization of the ZnO NR arrays is better on the sputtered layer than on the sol-gel process layer.

As well as the XRD measurement of the seed layer, the μ-PL spectra of NRs are also measured. **Figure 4** shows the PL spectra of the NR arrays with different deposition methods. The emission peak at 385 nm originates from the excitonic recombination[19]. On the other hand, the green emission of the spectra comes from oxygen vacancies (intrinsic defects), again implying that the film quality of the sputtered layer is better than the quality of film formed by the sol-gel method. It can be noticed that the PL spectra of the ZnO NRs on sputtered AZO shows a considerably weaker peak at 385 nm compared to that of the ZnO NRs on sol-gel ZnO. This significant PL quenching occurs in the ZnO NR array on the sputtered AZO seed layer, implying that the AZO seed layer contains better exciton dissociation and charge separation capability than that of the ZnO sol-gel seed layer. The results reveal that the AZO/ZnO NRs layer based on the sputtering process appears to be a better electron transport layer than that based on the solution process.

Figure 5 shows the J-V characteristics of the devices with a sputtered AZO seed layer and a sol-gel processed ZnO seed layer. The short circuit current J_{sc}, open circuit voltage V_{oc}, FF, and the PCE can be derived from the J-V curves. The devices with a sputtered seed layer exhibit J_{sc} of 11.96 mA/cm^2, V_{oc} of 0.87 V, FF of 57.8%, and PCE of 6.01%, which is better than the sol-gel processed solar cell with J_{sc} of 10.01 mA/cm^2, V_{oc} of 0.88 V, FF of 53.8%, and PCE of 4.74%.

Table 1 shows the performance of the devices with different seed layers. By utilizing the sputtered seed layer, well-aligned vertically oriented ZnO NR ETL can be formed, and thereby not only the absorption but also the carrier collection efficiency can be enhanced. As a result, compared with the sol-gel processed devices, devices with a sputtered seed layer exhibit higher J_{sc} value (11.96 mA/cm^2) and better FF value (57.8%), as shown in **Table 1**.

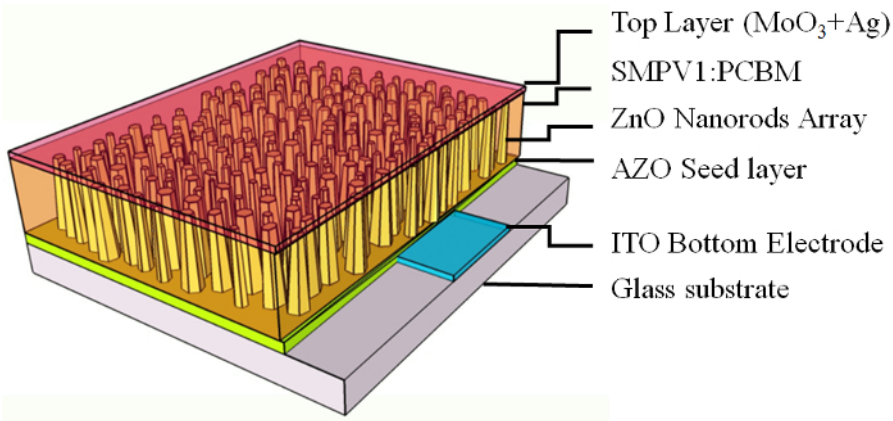

Figure 1: Schematic diagram of the inverted small molecule solar cell structure. Layered structure of the devices consisted of ITO substrate/AZO (40 nm)/ZnO NRs layer, SMPV1:$PC_{71}BM$ (80 nm)/MoO_3 (5 nm)/Ag (150 nm). Please click here to view a larger version of this figure.

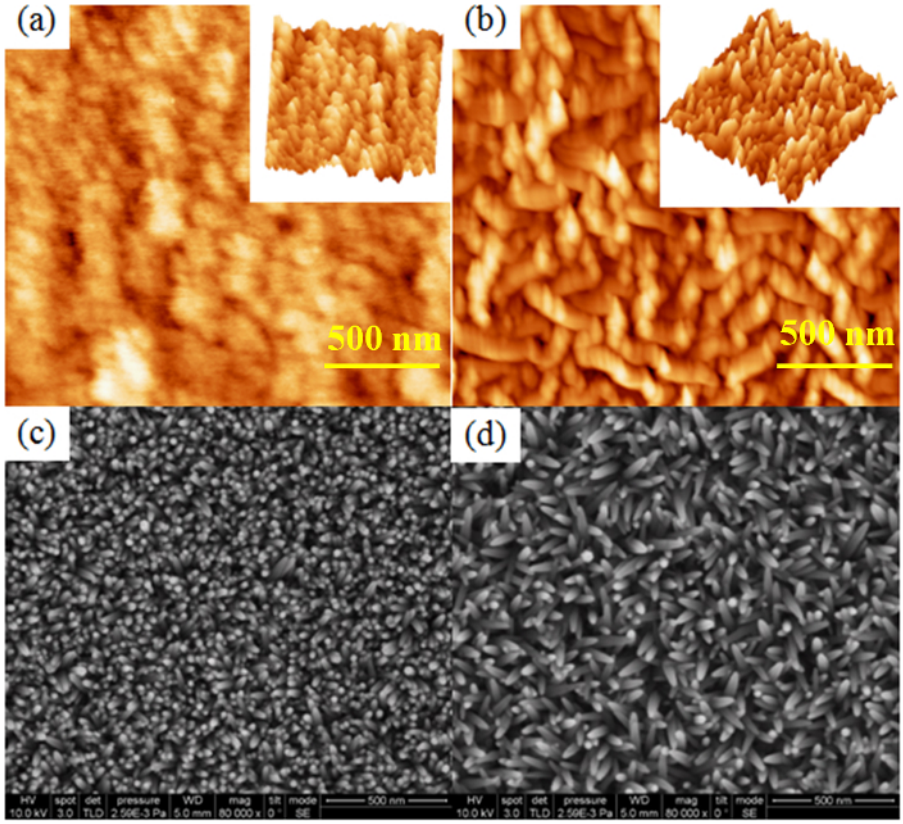

Figure 2: AFM and SEM images of ZnO NR array. AFM images of ZnO NR array grown on (**a**) a sputtered AZO seed layer and (**b**) a sol-gel processed ZnO seed layer; SEM top-view images of ZnO NR array grown on (**c**) a sputtered AZO seed layer and (**d**) a sol-gel processed ZnO seed layer. The surface morphology and roughness of the ZnO NRs layer can be observed via the AFM and SEM images. Please click here to view a larger version of this figure.

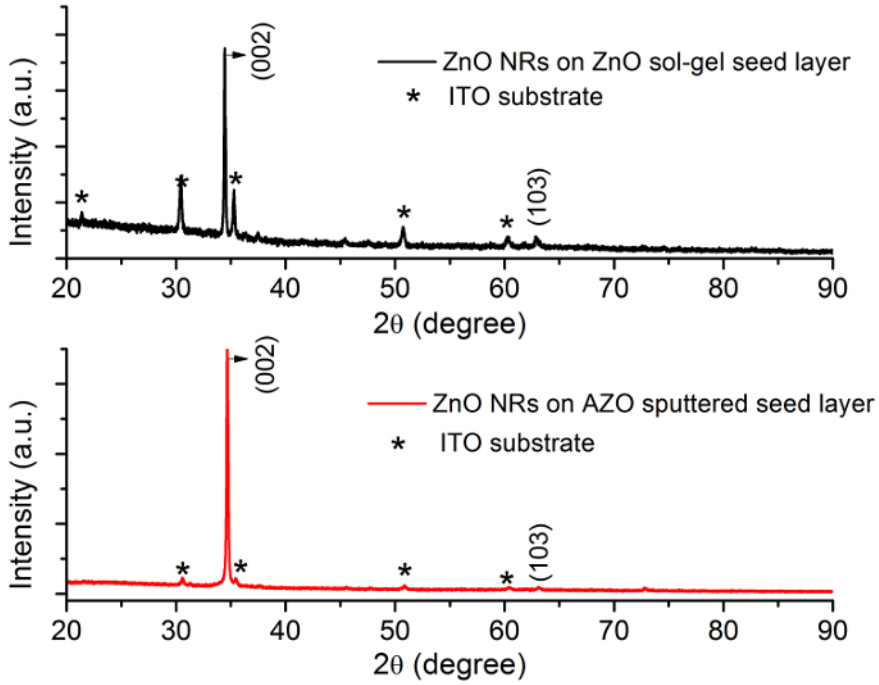

Figure 3: XRD spectra of ZnO NR array. The XRD pattern of ZnO NR array grown on a sputtered AZO seed layer and a sol-gel processed ZnO seed layer. The orientation and crystallization of the NRs can be identified by the XRD spectra. The ZnO NR array grown on different seed layers exhibits almost the same orientation (002). The strength of the (002) peak for the NRs on sputtered AZO seed layer is stronger than that on sol-gel processed ZnO seed layer, revealing that the ZnO NRs on sputtered AZO seed layer exhibits better vertical orientation along the (002) axis. Please click here to view a larger version of this figure.

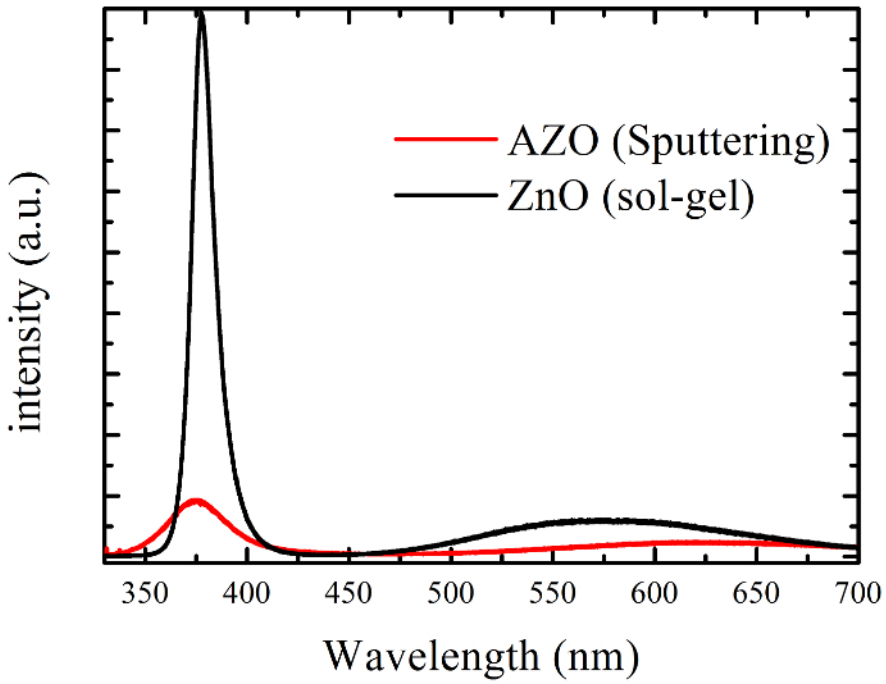

Figure 4: PL spectra of AZO and ZnO seed layer. The PL spectra of a sputtered AZO seed layer and a sol-gel processed ZnO seed layer. The defects and the exciton dissociation capability of the NRs can be evaluated by the PL spectra. The emission peak at 385 nm originates from the excitonic recombination and the green emission of the spectra comes from oxygen vacancies of the ZnO NR array. Please click here to view a larger version of this figure.

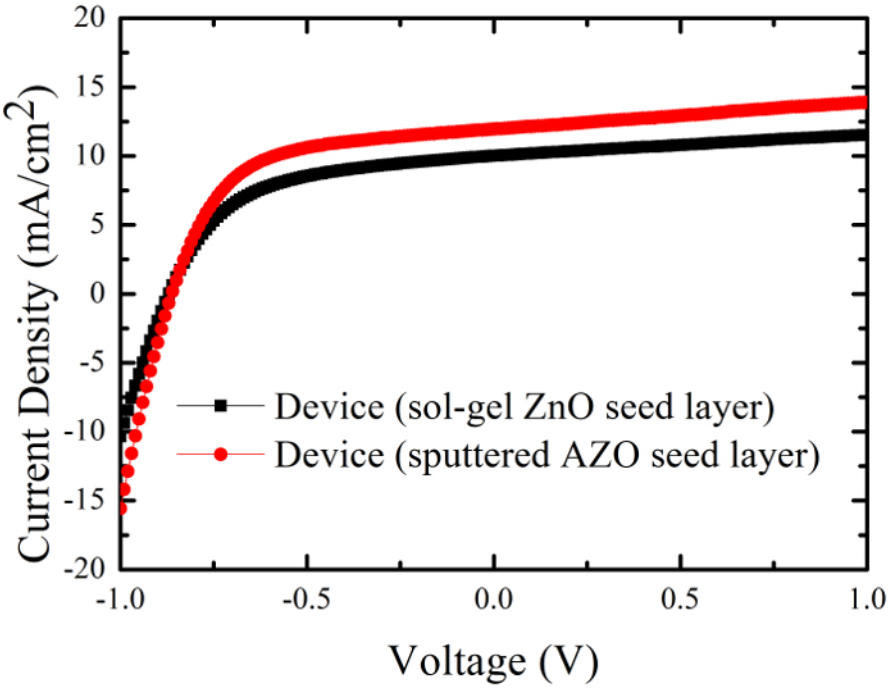

Figure 5: J-V curve of the devices with different seed layers. The J-V characteristics of devices under illumination with a sputtered AZO seed layer and a sol-gel processed ZnO seed layer. The performance of the solar cells can be derived from the J-V curves[14]. Please click here to view a larger version of this figure.

Devices	V_{oc} (V)	J_{sc} (mA/cm^2)	FF (%)	PCE(%)
Sputtering seed layer	0.87	11.96	57.8	6.01
Sol-gel processed seed layer	0.88	10.01	53.8	4.74

Table 1: The performance of the devices with different seed layers. A summary of the performance of the devices derived from J-V curves including short circuit current, open circuit voltage, fill factor, and the power conversion efficiency

Discussion

By utilizing the NRs interlayer, both the J_{sc} and the FF of the devices can be improved. However, the surface roughness of NRs will also influence the subsequent processes. Thus, the orientation and the surface morphology of the NRs should be carefully manipulated. For a long time, the sol-gel processed ETL such as TiO_2 and ZnO were commonly used in PSCs due to their simple procedures. However, the crystallization of sol-gel processed layers is generally of the amorphous type, and the surface morphology of the layers is rough in the majority of the cases. Hence, in this study, to precisely control the film quality of the seed layer, the sputtered seed layer has been selected to replace the sol-gel processed seed layer. The ZnO NRs grown on the sputtered AZO seed layer also show better vertical alignment, which is beneficial for subsequent processes. It is noted that at the end of the NRs growth process, the residual precursor solvent on the NRs needs to be removed, and thus the sample needs to be baked on the hot plate to ensure the residual solvent dries out completely. Furthermore, to avoid the annealing effect changing the surface morphology, the drying temperature is set at 250 °C, which is below the recrystallization temperature of the ZnO.

In general, the transport layer of the OPV devices dominates the carrier collection and transportation of the solar cells. As a result, improving the mobility of the transport layers is very critical[9]. Unlike the sol-gel processed film, by adjusting the RF power, deposition temperature, and doping concentration of the AZO target, the sputtered AZO seed layer film can maintain high crystallization and high electron mobility.

Even under various environments or conditions of this fabrication process, it is still easy to replicate the results of the experiment. As long as the film quality of the seed layer is well controlled, the well-aligned vertically oriented ZnO NR array can be easily obtained.

Although the ZnO NR array shows great potential to function as ETL in OPVs, the sheet resistance of the ZnO NR array is still high. Hence, the ZnO NR arrays cannot replace the ITO and need to be compatible with ITO or other transparent electrodes during the applications.

Other than functioning as the ETL in the SM-OPVs, the well-aligned vertically oriented ZnO NR arrays can also work as an anti-reflection layer in an organic light-emitting diode (OLED) to increase light emission[20]. Moreover, for illumination applications, it can function as a donor to recombine with holes to emit light of a specific wavelength[21]. Consequently, we believe that high quality sputtered AZO film and well-aligned vertically oriented ZnO NR arrays will play an important role in the optoelectronics industry in the future.

Disclosures

The authors declare that they have no competing financial interests.

Acknowledgements

The authors would like to thank the National Science Council of China for the financial support of this research under Contract No. MOST 106-2221-E-239-035, and MOST 106-2119-M-033-00.

References

1. Dou, L., *et al.* Tandem polymer solar cells featuring a spectrally matched low-bandgap polymer. *Nat. Photonics.* **6**(3), 180-185 (2012).
2. You, J., *et al.* Metal Oxide Nanoparticles as an Electron-Transport Layer in High Performance and Stable Inverted Polymer Solar Cells. *Adv. Mater.* **24**(38), 5267-5272 (2012).
3. Dou, L., *et al.* Systematic Investigation of Benzodithiophene- and Diketopyrrolopyrrole-Based Low-Bandgap Polymers Designed for Single Junction and Tandem Polymer Solar Cells. *J. Am. Chem. Soc.* **134**(24), 10071-10079 (2012).
4. Li, G., Zhu, R., Yang, Y. Polymer solar cells. *Nat. Photonics.* **6**(3), 153-161 (2012).
5. You, J., *et al.* A polymer tandem solar cell with 10.6% power conversion efficiency. *Nat. Commun.* **4**, 1446 (2013).
6. Chen, J. D., *et al.* Single-Junction Polymer Solar Cells Exceeding 10% Power Conversion Efficiency. *Adv. Mater.* **27**(6), 1035-1041 (2015).
7. Zhang, H., *et al.* Developing high-performance small molecule organic solar cells via a large planar structure and an electron-withdrawing central unit. *Chem. Commun.* **53**, 451-454 (2017).
8. Zhou, H., *et al.* Conductive Conjugated Polyelectrolyte as Hole-Transporting Layer for Organic Bulk Heterojunction Solar Cells. *Adv. Mater.* **26**(5), 780-785 (2014).
9. Lin, M. Y., *et al.* Enhance the light-harvesting capability of the ITO-free inverted small molecule solar cell by ZnO nanorods. *Opt. Express.* **24**(16), 17910-17915 (2016).
10. Liu, Y., *et al.* Solution-processed small-molecule solar cells: breaking the 10% power conversion efficiency. *Sci. Rep.* **3**, 3356 (2013).
11. Farahat, M. E., *et al.* Toward environmentally compatible molecular solar cells processed from halogen-free solvents. *J. Mater. Chem. A Mater. Energy Sustain.* **4**(19), 7341-7351 (2016).
12. Lin, M. Y., *et al.* Plasmonic ITO-free polymer solar cell. *Opt. Express.* **22**(S2), A438-A445 (2014).
13. Donato, A., *et al.* RF sputtered ZnO-ITO films for high temperature CO sensors. *Thin Solid Films.* **517**(22), 6184-6187 (2009).
14. Lin, M. Y., *et al.* Sol-gel processed CuOx thin film as an anode interlayer for inverted polymer solar cells. *Org. Electron.* **11**(11), 1828-1834 (2010).
15. Vandewal, K., *et al.* On the origin of the open-circuit voltage of polymer-fullerene solar cells. *Nat. Mater.* **8**, 904 - 909 (2009).
16. Sharma, R., *et al.* X-ray diffraction: a powerful method of characterizing nanomaterials. *Recent Research in Science and Technology.* **4**(8), 77-79, (2012).
17. Huggett, J. M., Shaw H. F. Field emission scanning electron microscopy a high-resolution technique for the study of clay minerals in sediments. *Clay Miner.* **32**, 197-203 (1997).
18. Lou, S., *et al.* Laser beam homogenizing system design for photoluminescence. *Appl. Opt.* **53**(21), 4637-4644 (2014).
19. Huang, J. S., & Lin, C. F. Influences of ZnO sol-gel thin film characteristics on ZnO nanowire arrays prepared at low temperature using all solution-based processing. *J. Appl. Phys.* **103**, 014304 (2008).
20. Leung, S. F., *et al.* Light Management with Nanostructures for Optoelectronic Devices. *J. Phys. Chem. Lett.* **5**, 1479−1495 (2014).
21. Lee, C.Y., *et al.* White-light electroluminescence from ZnO nanorods/polyfluorene by solution-based growth. *Nanotechology.* **20**(42), 425202-1-425202-5 (2009).

